A room ventilation and heat transfer experimental facility

Stefan Hudjetz and Roland Koenigsdorff
Biberach University of Applied Sciences, Germany

Simon J. Rees and Malcolm J. Cook
De Montfort University Leicester, England

ABSTRACT

Energy-efficient building design often makes use of night-time ventilation or thermal slab activation. The quality of the design tools used depends on the quality of the empirical values used within them such as heat transfer coefficients. Thus, an experimental facility for investigation of room ventilation and indoor heat transfer has been built at Biberach University of Applied Sciences in Germany. Initial tests have been conducted investigating natural convection heat transfer with an electrical heating element on the floor. The facility, its instrumentation and initial experimental results are presented in this paper.

1. INTRODUCTION

Climate change, a growing demand for comfortable indoor environments and new national standards create the need for energy-efficient design concepts for buildings. Design tools, e.g. for night-time ventilation already exist. However, researchers strive to enhance such building design concepts using both simulation and monitoring data from completed projects (Pfafferott, 2004). For modelling convective heat transfer, correlations from experimental investigations are implemented into building simulation programs. Various correlations for indoor convective heat transfer can be found in literature (Khalifa, 2001a) (Khalifa, 2001b). Some of these will be shown in section 5.2. However, many of these correlations are not suitable for building technology applications. In (Pfafferott et al., 2005), the authors point out that heat transfer near the ceiling needs further investigation for strategies using thermal slab activation. Thus, an experimental facility for investigating room ventilation and heat transfer has been built at Biberach University of Applied Sciences.

2. OBJECTIVES

The aim of the investigations of room ventilation and heat transfer in the experimental facility is the creation of an empirical database of heat transfer coefficients for different applications (e.g. thermal slab activation or night-time ventilation and the effect on heat transfer caused by obstacles in the room) and for validation of simulation models such as those developed by Zitzmann et al (2007). Based on these data, guidelines for determining the thermal performance of rooms can be developed.

3. FACILITY AND INSTRUMENTATION

3.1 Description of the test chamber

The experimental facility consists of an insulated cabin which was built in the corner of a laboratory room and has internal dimensions of 2.30 m in length, 1.65 m in width and 2.25 m in height. All walls are made of two different types of insulation material. One is a Polyurethane sandwich element with paper-clad aluminium foil on both sides. Its thickness is 0.02 m and conductivity is 0.025 $Wm^{-1} K^{-1}$. The second material comprises plates made of Styrodur® with a thickness of 0.05 m and a conductivity of 0.035 $W m^{-1} K^{-1}$. The composition of the enclosing surfaces is displayed in Figures 1 to 3.

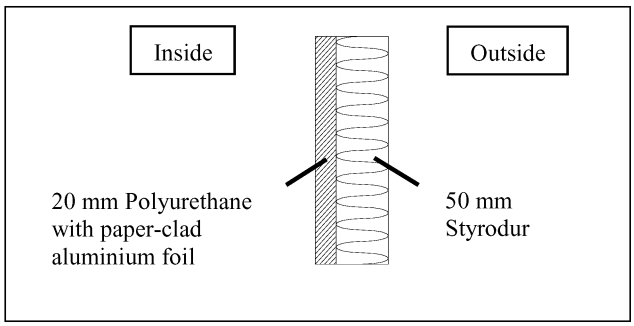

Figure 1. Composition of front, rear and sidewalls.

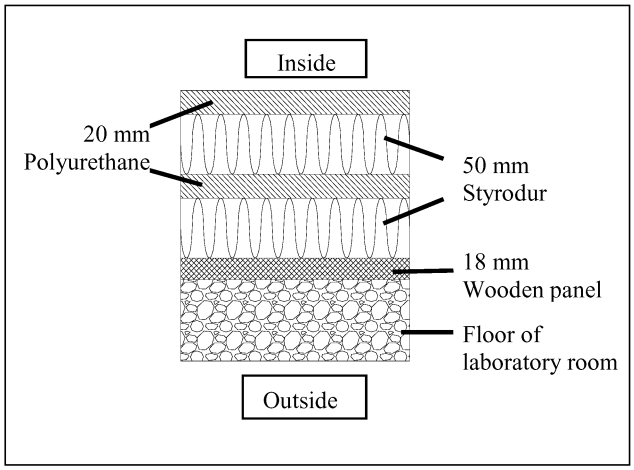

Figure 2. Composition of floor.

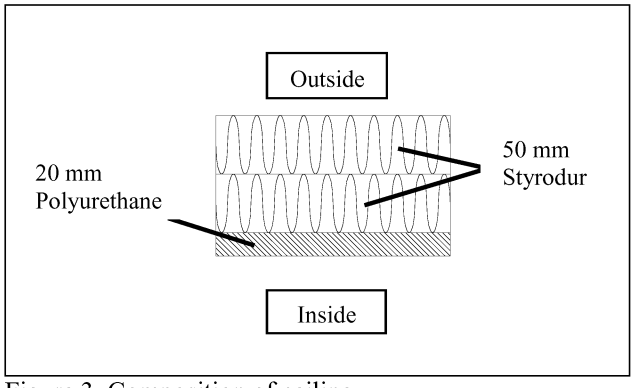

Figure 3. Composition of ceiling.

The cabin can be ventilated via a slot inlet positioned close to the floor. The outlet is located in the same wall at high level below the ceiling, thus facilitating single-sided ventilation. Other opening configurations are planned for subsequent tests. A tracer gas system is available for measuring air exchange rates and age of air. Initial tracer gas experiments confirmed that the cabin is almost completely airtight due to the paper-clad aluminium foil and the sealed joints. The ventilation system and its components, the heat source, the data acquisition system and the installed sensors are described in more detail in the following sections.

3.2 Ventilation system

Single-sided ventilation with openings at high and low level can be investigated in the test chamber. Supply air can either be heated or cooled with a heat exchanger. The air flow rates can be measured with a rotating vane anemometer. In order to be able to obtain quasi-2D situations in the cabin, the supply air is delivered to the room via a slot inlet that covers the full width of the cabin. The system and its components are shown in figure 4.

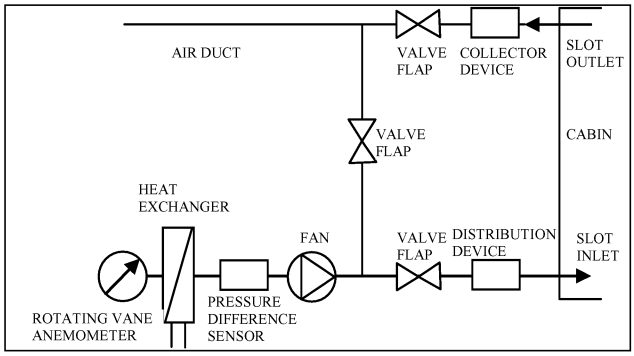

Figure 4. Components of the ventilation system.

3.3 Electrical heating element

The cabin can be heated with an electrical heating plate which was mounted on the floor for the experiments described in this paper for investigation of heat transfer from its surface to the room. An EB-THERM rectangular film electrical heating element with a width of 0.60 m and a length of 1.65 m was used as the heat source. The film element is embedded between copper plates for uniform temperature distribution on the surface. Heat output of the element can be adjusted with a DC-regulated dimmer and constantly monitored using a ZES LMG95 high-precision power meter as shown in figure 5. The heat output ranges from approximately 30 Watts up to 270 Watts.

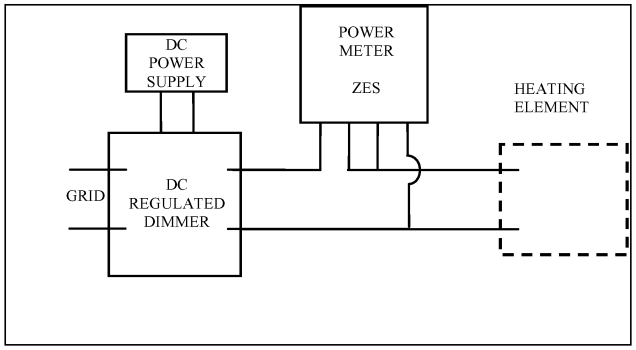

Figure 5. Electrical heating element and instrumentation.

3.4 Data acquisition

For data acquisition and logging, an Agilent 34970A data acquisition/switch unit is used. As plug-in modules, Agilent's 34901A 20-channel-multiplexer cards are employed. All resistance temperature sensors are connected in four-wire configuration to Printed Circuit Boards (PCBs) which provide a constant current for the sensors. The PCBs are connected to the multiplexer cards for recording the temperature-dependent voltage signal. All data is collected at 30s intervals.

3.5 Air and surface temperature measurement

Air and surface temperatures are measured using two types of platinum resistance thermometers (PRTs). The first type are Platinum-chip sensors (CPRTs) offering a resistance of 100 Ohm at 0 °C (Pt100) with a tolerance class of 1/3 DIN B (according to DIN EN 60751). The second type are Platinum-foil sensors (FPRTs) (also Pt100) with tolerance class B.

For each wall, surface temperatures are measured at six different points. The positions of the sensors are shown in figure 6.

An additional 12 sensors (6 CPRTs and 6 FPRTs) are used for measuring indoor air temperatures at different locations. A further six sensors (FPRTs) are installed for measuring the heat loss of the cabin due to conduction to the backside of the insulation.

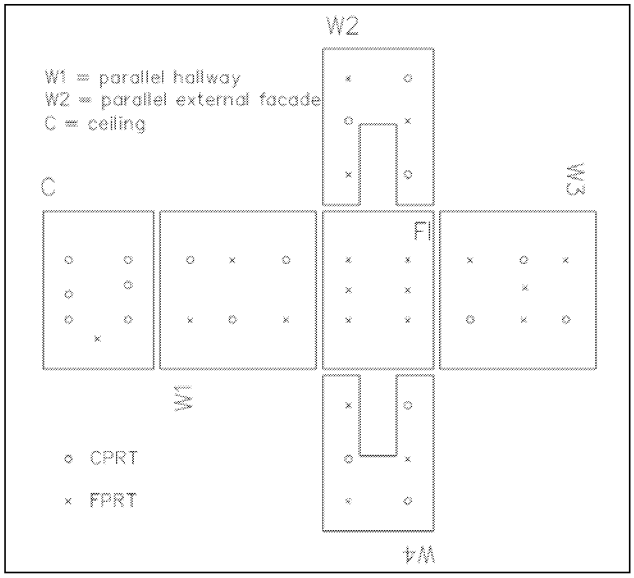

Figure 6. Net view of the cabin.

3.6 Tracer gas system

For tracer gas measurements an AUTOTRAC® 101 automatic tracer gas monitor from Lagus Applied Technology, Inc. is available. The tracer gas monitor is configured for sulphur hexafluoride, SF_6, and is equipped with an internal 8-port automatic sampling module. Precision of the monitor is specified by the manufacturer to be better than ±3% of the reading within the linear dynamic range from 0.05 to 50 ppb. For air flow rate measurements an optional flow rate measurement kit is also available.

4. EXPERIMENTAL UNCERTAINTIES

4.1 Temperature measurement

Before installing the temperature sensors in the test chamber, the complete temperature measurement system was calibrated. Each of the installed PRTs was calibrated twice with multiple readings for each calibration in a temperature band from 15 °C to 45 °C using high-precision mercury-in-glass thermometers as a reference and a calibration bath system. The remaining uncertainty in temperature measurement, after the calibration process, is defined by the uncertainty of the mercury-in-glass-thermometers, the inaccuracy in reading the scale of the mercury-in-glass thermometer, the maximum deviation of the measured data from the resulting calibration curve used for correcting each sensor signal, the long-term stability of the sensors and the

repeatability of the measurement which is described below.

The uncertainty of the mercury-in-glass thermometers is certified to not exceed 0.01 K. The inaccuracy in reading the thermometer is equal to half of the smallest subdivisions of the thermometer, thus being 0.005 K. The maximum deviation between the single read values and the calibration curves is 0.13 K. The long-term stability of the sensors is given by the manufacturer to be below 0.25 K. The deviation between the two calibration tests, and thus the repeatability of the measurement, was found to be a maximum of 0.12 K. The latter number was obtained by subtracting the average errors of the second calibration from the average errors of the first calibration. The resulting mean of the deviations between the two calibration tests of the Chip-PRTs is 0.015 K and the standard deviation is 0.017 K. The arithmetic mean of the average error differences of the foil sensors is 0.07 K with a standard deviation of 0.05 K. Adding those two values yields the maximum deviation of 0.12 K between the two calibration tests mentioned above.

Since the individual errors are considered as random and independent, they can be added in quadrature (Spitler et al., 1991). Hence, the resulting total uncertainty of both the surface and air temperature measurement system after the calibration was ±0.3 K.

4.2 Power measurement

Electrical power is monitored continuously during the experiments. Accuracy of the high-precision power meter is given as 0.015% of the reading plus 0.02% of the range. For the power output achievable with the heating element and the selected measuring range this leads to an uncertainty in power measurement which is below 1% of the measured values.

4.3 Flow rate measurement

Air flow rates were measured using a large rotating vane anemometer (sensor diameter 11cm). The recommended operating conditions range from 6 m^3/h to 130 m^3/h. This leads to possible air change rates in the cabin that can be measured accurately of between 1 ach^{-1} and 15 ach^{-1}. The accuracy of the anemometer is specified with 1% of the measured value ± 0.47 m^3/h.

5. INITIAL EXPERIMENTAL RESULTS

5.1 Experimental results for natural convection

A first set of experiments for investigation of room heat transfer without ventilation was conducted with the electrical heating element placed on the centre of the floor covering the whole width of the cabin. The heat output of the element was set to a constant value and experiments were run until steady-state conditions were achieved. The heat output was in the range from 30 W to 275 W. Conductive loss at the back of the element was calculated using the temperatures measured. Due to the good insulation, these conduction losses play a minor role with values ranging between 3% and 9% of the heat output of the heating element. Radiative heat flux from the heating element to the enclosing surfaces was calculated using the formulae for a cavity with two zones including multiple reflections (Modest, 2003). In this case, radiative flux from the heating element can be written as

$$\dot{Q}_{rad} = \varepsilon_{12} \cdot A_1 \cdot \sigma \cdot \left(T_1^4 - T_2^4\right) \qquad (1)$$

where
Q_{rad} = radiative heat flux in [W]
A_1 = area of heating element in [m^2]
σ = Stefan-Boltzmann constant [W m^{-2} K^{-4}]
T_1 = temperature of heating element in [K]
T_2 = temperature of enclosing surfaces in [K]
ε_{12} = emissivity which can be calculated using equation (2).

$$\frac{1}{\varepsilon_{12}} = \frac{1}{\varepsilon_1} + \frac{A_1}{A_2} \cdot \left(\frac{1}{\varepsilon_2} - 1\right) \qquad (2)$$

where
ε_1 = emissivity of heating element in [-]
ε_2 = emissivity of enclosing surfaces in [-]
A_1 = surface area of heating element in [m^2]
A_2 = surface area of enclosing surfaces in [m^2]

A value of 0.9 was used for both the heating element and enclosing surfaces emissivity.

This analytic approach for calculating radiation shows good agreement with detailed modelling of radiative heat transfer in a model of the cabin

using computational fluid dynamics (CFD) in (Pfrommer, 2008).

The remaining convective part of the heat flux was determined by subtracting radiation and conduction from the measured heated plate output. Convective heat transfer coefficients (CHTCs) for the hot plate were calculated using equation (3) and the averaged room air temperature measured at nine different locations within the cabin as reference temperature. The results are displayed in Figure 7.

$$h_c = \frac{\dot{q}_{conv}}{T_{surf} - T_{ref}} \tag{3}$$

where
h_c = CHTC in [W m^{-2} K^{-1}]
q_{conv} = convective heat flux in [W m^{-2}]
T_{surf} = surface temperature in [°C]
T_{ref} = reference temperature in [°C]

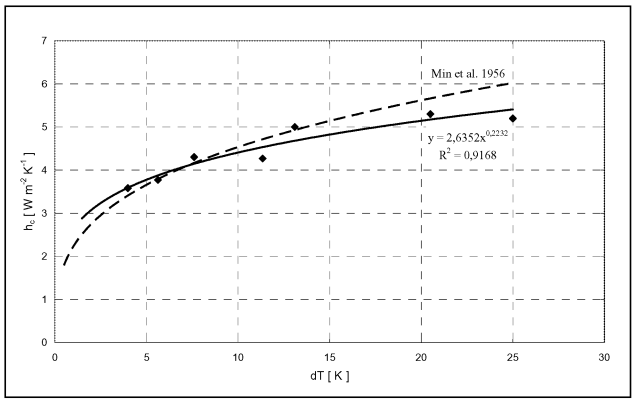

Figure 7. CHTCs for various temperature differences.

Plotting a curve fit for the above results leads to the following equation:

$$h_c = 2.635 \cdot (dT)^{0.2232} \tag{4}$$

where *dT* is the difference between the hot plate surface and the mean air temperature.

5.2 Comparison with existing correlations

Khalifa conducted an extensive review of natural convective heat transfer coefficients both on isolated surfaces and in two- and three-dimensional enclosures (Khalifa, 2001a) and (Khalifa, 2001b). In (Khalifa, 2001b), the author presents correlations for a heated plate facing upward by plotting h vs. dT for temperature differences up to 10 K.

Figure 8 shows the correlations given by Khalifa and the experimental results presented above. The discrepancies between the correlations shown are found to be up to a factor of 4. It can be seen that for temperature differences below 10 K, the results from this research show good agreement with those of Min et al. (1956) who investigated a chamber with heated panels. Min et al.'s correlation which can be expressed using equation (5) is also shown in Figure 7 for temperature differences up to 25 K.

$$h = 2.416 \cdot (dT)^{0,31} / D_e^{0.08} \tag{5}$$

where *dT* is the temperature difference of the surface and the room air and D_e is the equivalent diameter which equals four times the area divided by the perimeter length.

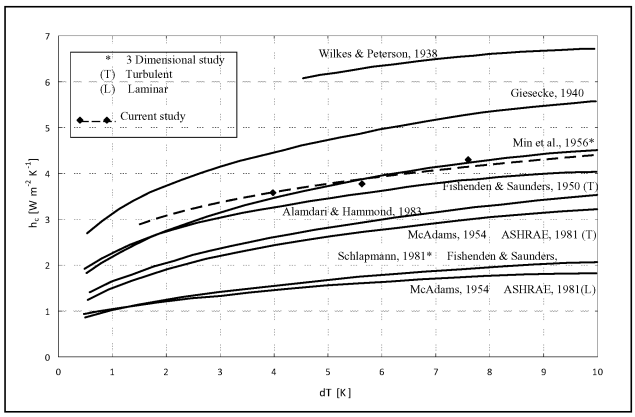

Figure 8. Natural convection heat transfer correlations for heated floors given in literature and first results of this research.

6. CONCLUSIONS AND OUTLOOK

A wide range of correlations for natural heat transfer coefficients exist. Many of those were obtained from experiments on isolated surfaces and thus are not suitable for application in building analysis and design. Therefore, a new test chamber has been built at Biberach University of Applied Sciences in Germany to investigate surface heat transfer in buildings. Initial results for an unventilated chamber and heated floor are presented in this paper and correlate well with experimental work of Min et al.

(1956) who used a panel-heated chamber. These initial results will be subject to closer scrutiny as the project progresses. In subsequent tests, correlations for a heated plate at the ceiling (facing downwards), as well as different ventilation cases, will be investigated.

ACKNOWLEDGEMENTS

This work was funded by the German Federal Ministry of Education and Research (research grant number 1749A04).

REFERENCES

Alamdari F, Hammond GP (1983). Improved data correlations for buoyancy-driven convection in rooms. Build Serv Engng Res Technol, 4:106-12.

ASHRAE Handbook of Fundamentals, 1981.

Fishenden M, Saunders OA (1950). An introduction to heat transfer. Oxford: Clarendon Press.

Giesecke FE (1940). Radiant heating and cooling. ASHVE, J, Heating Piping Air Cond, 12:484-5

Khalifa A-J N (2001a). Natural convective heat transfer coefficient – a review I. isolated vertical and horizontal surfaces. Energy Conversion & Management, 42:491-504.

Khalifa A-J N (2001b). Natural convective heat transfer coefficient – a review II. Surfaces in two- and three-dimensional enclosures. Energy Conversion & Management, 42: 653-661.

McAdams WH (1954). Heat transmission. New York: McGraw-Hill.

Min TC, Schutrum LF, Parmelee GV, Vouris JD (1956). Natural convection and radiation in a panel-heated room. ASHRAE Trans, 62:337-58

Modest MF (2003). Radiative Heat Transfer. Academic Press, Second Edition, ISBN-10: 0125031637

Pfafferott J (2004). Enhancing the Design and the Operation of Passive Cooling Concepts: Monitoring and Data Analysis in Four Low-Energy Office Buildings with Night Ventilation. PhD thesis, Fraunhofer-Institut für Solare Energiesysteme ISE, Freiburg.

Pfafferott J, Schiel S and Herkel S (2005). Bauteilkühlung. Messungen und modellbasierte Auswertung. Tagungsband 15. Symposium Thermische Solarenergie, OTTI-Energie-Kolleg, Staffelstein

Pfrommer P (2008). Simulation und Optimierung des thermischen Austausches zwischen Massivbauteilen und Raumluft mit CFD-Modellen. Schlussbericht.

Schlapmann D (1981). Convection with floor heating-development of a test method. Report No. BMFT FB-T 81-158, Universität Stuttgart, 7000 Stuttgart 80, Sept. 1981.

Spitler J, C Pedersen, D Fisher, P Menne, J Cantillo (1991). An Experimental Facility for Investigation of Interior Convective Heat Transfer, ASHRAE Transactions. 97(1): 497-504.

Wilkes GB, Peterson CMF (1938). Radiation and convection from surfaces in various positions. ASHVE Research Report, No. 1098, ASHVE Trans, 44:515-20.

Zitzmann T (2007). Adaptive Modelling of Dynamic Conjugate Heat Transfer and Air Movement using Computational Fluid Dynamics. PhD thesis, De Montfort University, Leicester.